PAPER VII

Quantum Seed and Packet Calculus

Symmetry, circuits, geometric transport, channels, and effective dynamics

Forty worked and reference pages follow quantum seeds, coherent circuit paths, moving subspaces, channels, error recovery, hidden dynamics, and the hypotheses needed for continuum limits.

Komorebi P.

Visual guide • 18 October 2026

How to use this volume

Follow each small model through its matrices and formulas, then read the cited general argument in the traditional volume. The Lean companion records the formal statements and their precise hypotheses.

Routes through the guide

The labels V1 through V40 identify worked pages independently of PDF pagination. The source line below each title points into the strengthened quantum development in Traditional Part II. The traditional volume also retains the corrected finite core and the completion supplements as distinct branches.

Route	Mathematical question	Visual pages
Seeds and symmetry	Which algebra and multiplicities determine the generated span?	1–7, 29
Coherent circuits	Which amplitudes interfere before an outcome is measured?	8–11, 27
Moving subspaces	How do transport, local charts, and curvature enter?	12–15, 30
Channels and recovery	What survives dephasing and which errors can be corrected?	16–20, 31–33
Hidden dynamics	What self-energy and memory return after elimination?	21–23, 34–36
Limits and constraints	Which additional hypotheses support continuum passage?	24–26, 37–40
Evidence	What is checked, proved, or still open?	28, 40

Keep the operation visible

A complete packet decomposition retains the vector. Measurement and dephasing can remove coherence. Eliminating hidden states produces an exact memory equation, while deleting their coupling usually produces a different model.

A finite example checks its specified matrices or formulas. A written theorem gives an argument under quantified assumptions. A compiled Lean theorem certifies its formal statement in the recorded environment. The reading links help compare these accounts while keeping their hypotheses and evidence scopes distinct.

Preservation and evidence

The first 28 worked pages retain the mathematical content of the original appendix. Twelve further pages explain the strengthened results. All 38 editable TikZ plates and their Python generators remain available. The retained execution records describe the example suites, their tested inputs, and their rejected controls. This revision improves the prose and layout without presenting those earlier checks as new executions.

The inherited v0.6.0 formal ledger has 19 scoped finite results. The broader quantum development retains its written hypotheses, and the five continuum research targets remain open. The examples explain how the finite results work and where further arguments are needed.

Read this as: Choose a question, calculate its small model, and then check the hypotheses of the traditional result and the declared formal statement.

V1 / HOW TO READ THIS APPENDIX

Three objects, three questions

Traditional pp. 33, 50, 60 / Section II.1, Section II.7, Section II.9.

A quantum calculation becomes easier to follow when its objects remain visible. This appendix follows a state vector, a density matrix, and a retained part of a dynamical system. They may describe the same experiment, but they do not answer the same question.

$\sqrt{2}\,\psi$

1
0
0
1

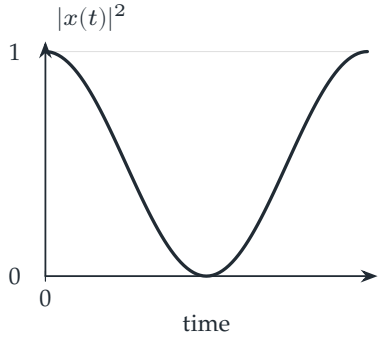
Two amplitudes one pure state

$2\rho = 2\psi\psi^*$

1	0	0	1
0	0	0	0
0	0	0	0
1	0	0	1

Off-diagonal entries retain phase.

Hidden coupling returns.



Amplitudes retain relative phase

For the Bell vector $\psi = (|00\rangle + |11\rangle)/\sqrt{2}$, the two nonzero entries are amplitudes. The density matrix $\rho = \psi\psi^*$ also records coherence in its off-diagonal entries. Measurements that compare the two addresses can detect this coherence. Deleting those entries applies a physical channel and changes the state.

How hidden dynamics returns

When a Hamiltonian couples a retained state to a hidden state, the retained amplitude can leave and later return. Its exact equation then remembers the hidden coupling. A smaller matrix obtained by deleting rows and columns does not generally reproduce that equation.

A route through the paper

Pages V3–V10 develop seeds, symmetry, and coherent circuit paths. Pages V11–V15 track leakage and moving subspaces. Pages V16–V20 distinguish measurement, channels, and recovery. Pages V21–V27 follow hidden dynamics and finite geometric diagnostics.

Read this guide alongside the traditional volume. The first 28 worked pages retain the original appendix's examples and mathematical content, with source references updated to this edition. Pages V29–V40 develop additional strengthened results. The example checks and the inherited Lean certificates have separately recorded scopes.

> **Read this as:** A packet coordinate change preserves information. A measurement, dephasing operation, or truncation may not. Always identify which operation is actually being performed.

V2 / AN ATLAS OF TYPES AND CONVENTIONS

The objects on the page

Traditional pp. 35, 50 / Definition II.2.1, Definition II.7.1.

The same letter can stand for different kinds of data in different calculations. Keep the following types fixed while reading a formula. In this appendix, vectors are columns, operators compose from right to left, and A^* denotes the conjugate transpose.

Symbol	Object	What it records
$\mathcal{H}, \psi$	Hilbert space and state vector	They specify the space of addresses and its coherent amplitudes.
$\mathcal{A}$	Declared operator algebra	It specifies the available linear operations.
P_a	Orthogonal packet projector	It selects an entire subspace.
ρ	Positive matrix of trace one	It records populations and coherences.
E_k	Positive measurement effect	It gives the outcome probability $\mathrm{Tr}(E_k\rho)$.
K_a	Kraus operator	It describes one channel branch and need not be a projector.
H	Self-adjoint Hamiltonian	It generates evolution in real time through $e^{-\mathrm{i}tH}$.
C, ∇	Packet transport generator and connection	They describe moving subspaces and differentiation within their ranges.
P, Q	Retained and hidden projectors	They define a decomposition with $Q = I - P$.
$\Sigma(z)$	Self-energy	It records the spectral influence of the hidden sector.
$L, T(\tau)$	Nonnegative operator and Euclidean transfer	They determine decay factors and finite heat trace diagnostics.

Normalization and indexing

The tensor factors are ordered from left to right, so $X_1 = X \otimes I \otimes I$. A normalized pure state gives $\rho = \psi\psi^*$. A coefficient matrix used to count a seed orbit need not be normalized. Scaling a nonzero seed does not change its generated linear span.

A Hamiltonian and a Hadamard gate are both traditionally denoted H. Where both appear, the gate is H_{Had} and the Hamiltonian keeps the letter H. Numerical labels on a drawing are coordinates or exact example values, not observations of a physical device.

> **Read this as:** Check the type before interpreting the picture. An idempotent projector, a density matrix, and a channel matrix have different defining equations.

V3 / CYCLICITY DEPENDS ON THE GRAMMAR

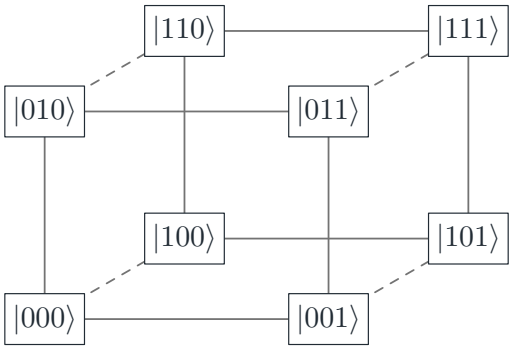
One seed, eight addresses

Traditional p. 37 / Proposition II.2.5.

Start with $\psi_0 = |000\rangle$ and allow the three bit flip operators X_1, X_2, X_3. For a binary address $a = (a_1, a_2, a_3)$, put

$$W_a = X_1^{a_1} X_2^{a_2} X_3^{a_3}. \qquad W_a \psi_0 = |a_1 a_2 a_3\rangle.$$

The drawing shows the actual eight states reached by these words. Dashed edges connect the two squares by changing the first bit. The other edges change one of the remaining bits.



Three actual words

$$W_{101} = X_1 X_3$$

$$W_{011} = X_2 X_3$$

$$W_{110} = X_1 X_2$$

$$\dim \operatorname{span}\{W_a |000\rangle\} = 8$$

Two different meanings of “reach”

The eight vectors are orthonormal, so their *linear span* is all of $\mathbb{C}^8$. This proves cyclicity for the algebra generated by the flips. Preparing every normalized vector requires more than products of these flips alone.

For example, no such word sends $|000\rangle$ to $(|000\rangle + |001\rangle)/\sqrt{2}$. A Hadamard gate, a suitable linear combination in the observable algebra, or a larger preparation grammar is required for that operation. Counting linearly independent addressed vectors and synthesizing a physical gate sequence are separate tasks.

The exact check constructs each 8×8 word matrix, applies it to the seed, and verifies that the matrix of all eight outputs is the identity. It also tests the displayed superposition against every word output. No search over an unspecified gate set is involved.

> **Read this as:** A cyclic seed generates a vector space under an algebra. That conclusion does not automatically provide a unitary preparation procedure for every vector in it.

V4 / SCHMIDT RANK AS ACCESSIBLE MULTIPLICITY

Entanglement changes the local span

Traditional p. 36 / Theorem II.2.2, Corollary II.2.4.

Write a bipartite vector as a coefficient matrix C, with the first subsystem indexing rows. Acting only on that subsystem transforms C to AC. Every resulting row remains in the row space of C, and every independent choice of such rows can be obtained in this way.

$$\dim \operatorname{span}\{(A \otimes I)\psi : A \in M_d(\mathbb{C})\} = d \operatorname{rank} C.$$

Product seed matrix

1	0
0	0

row rank 1
orbit dimension 2

Bell seed matrix $\sqrt{2}C$

1	0
0	1

row rank 2
orbit dimension 4

A acts on the left. It cannot invent a new direction in the row space.

The product vector $|00\rangle$ has matrix $C = \operatorname{diag}(1, 0)$. Its local orbit span allows arbitrary vectors in the first subsystem but only the second subsystem direction $|0\rangle$, so its dimension is two. The Bell vector has $C = I/\sqrt{2}$, rank two, and a four-dimensional local orbit span.

What the formula does not say

The action here allows arbitrary matrices and then takes a linear span. It is not the orbit under local unitary gates alone. Local unitary operations preserve Schmidt coefficients. They therefore cannot turn the Bell vector into an arbitrary product vector by a deterministic transformation between pure states.

For the exact calculation, apply the four matrix units E_{ab} to each seed matrix, flatten the outputs, and compute their column rank. The observed dimensions are two and four, respectively. The calculation directly exhibits the independent rows counted by the theorem.

> **Read this as:** Schmidt rank measures the remote multiplicity directions accessible to the local operator span. It is not permission for unrestricted deterministic local state preparation.

V5 / AN EXACT MULTIPLICITY LOWER BOUND

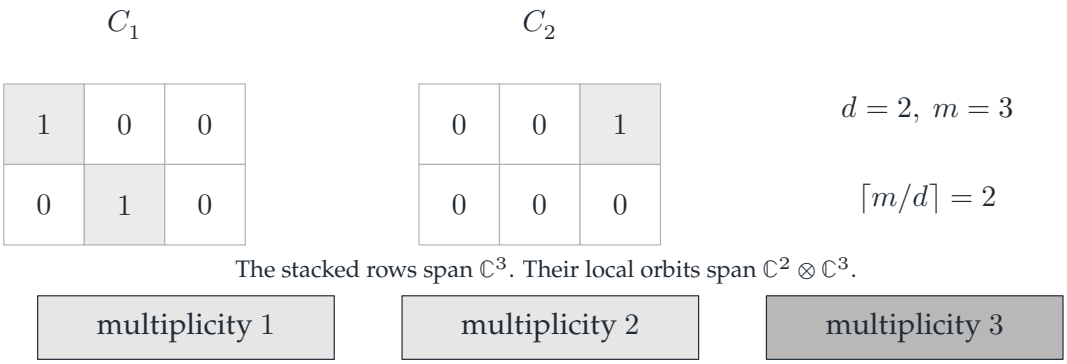
Why one seed is not always enough

Traditional p. 36 / Theorem II.2.3.

Consider $M_2(\mathbb{C}) \otimes I_3$ acting on $\mathbb{C}^2 \otimes \mathbb{C}^3$. A seed is a 2×3 coefficient matrix. Its two rows span at most two directions in the three-dimensional multiplicity factor. Therefore no single seed is cyclic for this algebra.

$$C_1 = \begin{pmatrix} 1 & 0 & 0 \\ 0 & 1 & 0 \end{pmatrix}, \qquad C_2 = \begin{pmatrix} 0 & 0 & 1 \\ 0 & 0 & 0 \end{pmatrix}.$$

These two matrices provide a complete set of row directions. Their individual orbit dimensions are four and two, and together those spans fill the six-dimensional state space.



From the example to the finite formula

For a block $M_d(\mathbb{C}) \otimes I_m$, k seed matrices contribute at most kd independent multiplicity directions. Hence $k \geq \lceil m/d \rceil$. Partitioning a multiplicity basis into groups of size at most d attains this bound. For a direct sum of such blocks, the worst block determines the required count:

$$\operatorname{srank}_{\mathcal{A}}(\mathcal{H}) = \max_i \lceil m_i/d_i \rceil.$$

This is an invariant of the declared representation of the algebra, and depends on more than the dimension of the Hilbert space alone. If the available algebra were enlarged to the full matrix algebra on $\mathbb{C}^6$, every nonzero seed would instead be cyclic.

The example checks both the ranks of the separate coefficient matrices and the rank three of their stacked row matrix. The argument explains why the construction meets the lower bound and therefore proves minimality.

> **Read this as:** Missing multiplicity directions cannot be created by reusing the same left action. Adding seeds and enlarging the operator algebra provide different ways to supply those directions.

V6 / CHARACTER PROJECTORS YOU CAN MULTIPLY

Four phases resolve a cyclic shift

Traditional p. 39 / Corollary II.3.3.

On four sites, let $S|k\rangle = |k+1 \bmod 4\rangle$ and let $\omega = \mathrm{i}$. The character projectors are the exact matrices

$$P_j = \frac{1}{4}\sum_{r=0}^{3} \mathrm{i}^{-jr} S^r, \qquad v_j(k) = \frac{1}{2}\mathrm{i}^{-jk}, \qquad P_j = v_j v_j^*.$$

All entries belong to the Gaussian rationals. Thus no approximation to a root of unity is needed in this model.

$2V$, with $V^*V = I$

	$j=0$	$j=1$	$j=2$	$j=3$
site 0	1	1	1	1
site 1	1	$-i$	-1	i
site 2	1	-1	1	-1
site 3	1	i	-1	$-i$

$$Sv_0 = 1v_0 \qquad P_0 = v_0 v_0^*$$

$$Sv_1 = iv_1 \qquad P_1 = v_1 v_1^*$$

$$Sv_2 = -1v_2 \qquad P_2 = v_2 v_2^*$$

$$Sv_3 = -iv_3 \qquad P_3 = v_3 v_3^*$$

Each column has four entries of magnitude $1/2$.

Reading the columns

Each column v_j is a normalized wave around the four sites. Advancing the address multiplies it by i^j. The entries show phase differences rather than four different probability distributions: every column has uniform site probability $1/4$.

Multiplying the actual projectors gives $P_j P_k = 0$ for $j \neq k$, $P_j^2 = P_j$, and $\sum_j P_j = I$. In particular, the complete packet tuple $(P_j\psi)_j$ retains the original vector exactly. Recording only the four packet norms is a different operation and can discard phase information between packets.

The same shift on four sites returns on V27, where it diagonalizes the Hamiltonian $L = 2I - S - S^*$, and its four character phases explain perfect transfer between opposite sites. The same fixed projectors serve as coordinates, symmetry sectors, and a complete interference ledger.

> **Read this as:** A character projector retains a complex subspace component. Its norm summarizes the size of that component while leaving its phase and direction unspecified.

V7 / TENSOR REFINEMENT BY TOTAL PARITY

A coarse packet can still contain coherence

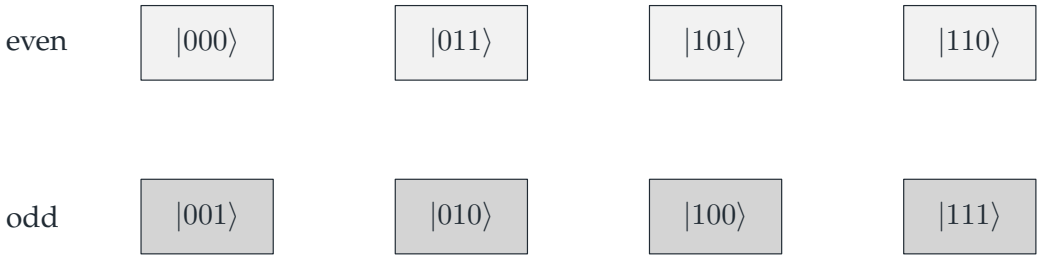
Traditional p. 40 / Theorem II.3.7, Corollary II.3.8.

For three qubits, the eight fine projectors are $P_a = |a\rangle\langle a|$. Grouping addresses according to the parity of their Hamming weight gives

$$P_{\text{even}} = P_{000} + P_{011} + P_{101} + P_{110} = \frac{I + Z \otimes Z \otimes Z}{2}, \qquad P_{\text{odd}} = I - P_{\text{even}}.$$

This is a sum of subspaces, not an averaging of their coordinates. The rank-four even packet retains all complex amplitudes on its four children.

Each coarse projector has rank four. All eight fine projectors have rank one.



Refinement is not measurement

The fine packet description and the coarse packet description each reconstruct the full vector when every component is retained. Replacing a state by the mixture $\sum_a P_a \rho P_a$ is instead a dephasing channel. That operation removes coherence between the fine packets and can differ from dephasing only between the even and odd sectors.

For instance, a superposition of $|000\rangle$ and $|011\rangle$ lies entirely in the even packet. Its internal relative phase survives a parity measurement but is lost by a complete measurement in the computational basis if outcomes are forgotten. The two measurements use projectors from the same refinement hierarchy but expose different information.

The exact check verifies all eight addresses, their parity grouping, the rank of both coarse projectors, and equality with the tensor expression above. The general residue version replaces parity by total label modulo N and groups the tensor descendants by their summed residue.

> **Read this as:** A coarse packet is a whole subspace. Internal coherence survives a change of address description. It is lost only when an operation discards it.

V8 / INTERMEDIATE PACKETS ARE NOT FINAL PACKETS

Track the Bell state through the circuit

Traditional pp. 41, 42 / Theorem II.4.1, Example II.4.6.

The input is $|00\rangle$. First apply a Hadamard to the first qubit, then a controlled flip:

$$|00\rangle \xrightarrow{H_{\text{Had}}\otimes I} \frac{|00\rangle + |10\rangle}{\sqrt{2}} \xrightarrow{\text{CNOT}} \frac{|00\rangle + |11\rangle}{\sqrt{2}}.$$

The displayed columns keep amplitudes, including their normalization, at every step. The middle vector occupies both parity packets. The final vector occupies only the even packet.

	seed
00	1
01	0
10	0
11	0

even only

	after $H \otimes I$
00	$\frac{\sqrt{2}}{2}$
01	0
10	$\frac{\sqrt{2}}{2}$
11	0

both parity packets

	after CNOT
00	$\frac{\sqrt{2}}{2}$
01	0
10	0
11	$\frac{\sqrt{2}}{2}$

even only, with coherence

How the exact path expansion works

Insert $P_{\text{even}} + P_{\text{odd}} = I$ between the two gates. Each summand records a particular intermediate packet, while the boundary projectors select its input and output packets. Summing all terms recovers the original 4×4 circuit matrix:

$$\sum_{a,b,c} P_b \,\text{CNOT}\, P_a (H_{\text{Had}} \otimes I) P_c = \text{CNOT}(H_{\text{Had}} \otimes I).$$

This expansion is an identity even though the intermediate parity is not measured. Physically inserting a measurement would alter the problem by removing interference between its alternatives. The derivation resolves intermediate coordinates without physically measuring them.

In the finite check, all eight matrix terms indexed by parity are constructed and summed. The matrix equality is checked before specializing to the input vector. It therefore verifies the decomposition for every input of this example, not merely agreement on the Bell seed.

> **Read this as:** A final invariant packet does not imply that each preceding gate preserved it. Follow the amplitudes through the actual intermediate resolutions.

V9 / HOW TWO PATH AMPLITUDES CANCEL

Why path probabilities do not add

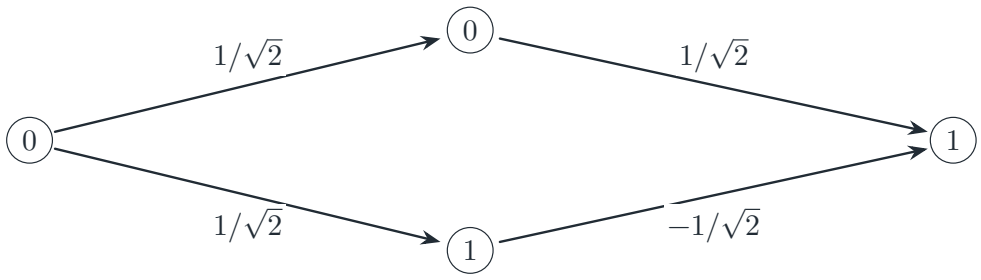
Traditional pp. 41, 42 / Theorem II.4.2, Theorem II.4.4.

Two consecutive Hadamard gates multiply to the identity. Starting from $|0\rangle$, there are two resolved paths to output $|1\rangle$. Their signed products are

$$\langle 1|H_{\mathrm{Had}}|0\rangle\langle 0|H_{\mathrm{Had}}|0\rangle = \frac{1}{2}, \qquad \langle 1|H_{\mathrm{Had}}|1\rangle\langle 1|H_{\mathrm{Had}}|0\rangle = -\frac{1}{2}.$$

Their sum is zero. Squaring each separately gives a different answer.

Two actual Hadamard paths, not classical alternatives



$$\text{amplitude} = 1/2 - 1/2 = 0 \quad \neq \quad \text{sum of path probabilities} = 1/2$$

Where the missing term goes

For path amplitudes a, b, the outcome probability is $|a+b|^2 = |a|^2 + |b|^2 + 2\Re(a\bar{b})$. Here the last term is $-1/2$, canceling the first two terms. The path picture retains this information only if its edges carry complex amplitudes rather than unsigned reachability or probabilities.

The packetwise unitarity identity is likewise an operator identity, including the off-diagonal cancellations:

$$\sum_b U_{ba}^* U_{bc} = \delta_{ac} P_a, \qquad U_{ba} = P_b U P_a.$$

It cannot be replaced by the assertion that every path individually has unit norm. The exact checks verify all four choices of a, c for the two rank-one packets, as well as the two path products leading to the opposite output.

A measurement at the intermediate stage would remove the cross term. In that modified experiment the two alternatives really would contribute total probability $1/2$ to output one. Adding the two path probabilities would therefore describe the experiment with an intermediate measurement.

> **Read this as:** Insert projectors algebraically to resolve paths, then add amplitudes. Add probabilities only when the physical setup has actually made the alternatives incoherent.

V10 / ONE HAMILTONIAN IN TWO ORDERS

A symmetry reveals blocks, not approximations

Traditional p. 43 / Theorem II.5.1.

Take the exact rational Hamiltonian

$$H = X \otimes X + \frac{3}{8}(Z \otimes I + I \otimes Z).$$

It commutes with total parity $Z \otimes Z$. Reordering the computational basis into even addresses $(00, 11)$ and odd addresses $(01, 10)$ displays the invariant subspaces explicitly.

Computational order

	00	01	10	11
00	$\frac{3}{4}$	0	0	1
01	0	0	1	0
10	0	1	0	0
11	1	0	0	$-\frac{3}{4}$

same operator
different order

Parity order

	00	11	01	10
00	$\frac{3}{4}$	1	0	0
11	1	$-\frac{3}{4}$	0	0
01	0	0	0	1
10	0	0	1	0

Even eigenvalues: $\pm 5/4$. Odd eigenvalues: ± 1.

$$H_{\text{even}} = \begin{pmatrix} 3/4 & 1 \\ 1 & -3/4 \end{pmatrix}, \qquad H_{\text{odd}} = \begin{pmatrix} 0 & 1 \\ 1 & 0 \end{pmatrix}.$$

The even block squares to $(25/16)I$, so its eigenvalues are $\pm 5/4$. The odd block squares to I, so its eigenvalues are ± 1. Exponentiating either block gives the corresponding part of the exact evolution. Transfer between the packets remains zero for every real time.

What has changed?

Only the order of basis vectors has changed. No matrix entries, amplitudes, or energy levels were discarded. This is why the decomposition is exact. Keeping just the even block would be a separate restriction of the state space, justified for initial data known to be even and for dynamics that preserve it.

The next page breaks a symmetry in a smaller model. There the entries coupling the packets no longer vanish, so their effect needs an explicit bound. The exact tests here multiply the commutator, verify the displayed permutation, and compute all four eigenvalues symbolically.

> **Read this as:** Block diagonalization uses an invariant decomposition already present in the operator. It is not evidence that an arbitrary chosen packet is invariant.

V11 / COMMUTATORS AND PROBABILITY BOUNDS

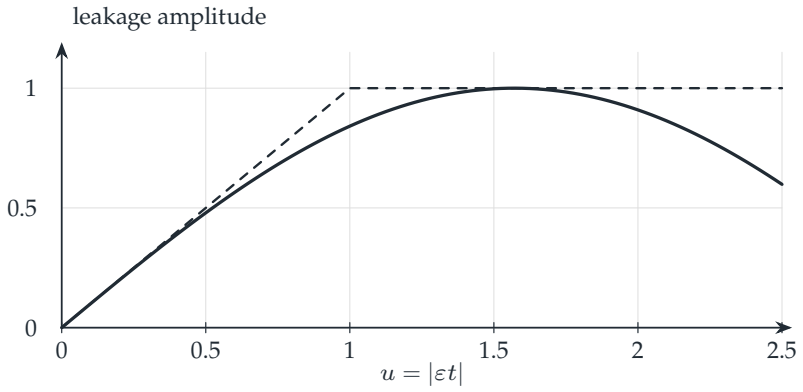
Quantify the amplitude that escapes

Traditional p. 44 / Theorem II.5.3, Corollary II.5.4.

For a two-level system, choose $H = \varepsilon X$, $P = |0\rangle\langle 0|$, and $Q = I - P$. Direct exponentiation gives

$$e^{-\mathrm{i}tH} = \cos(\varepsilon t)I - \mathrm{i}\sin(\varepsilon t)X, \quad \left\|Qe^{-\mathrm{i}tH}P\right\| = |\sin(\varepsilon t)|, \quad \|[H,P]\| = |\varepsilon|.$$

The general commutator estimate becomes the elementary bound $|\sin u| \le |u|$. Unitarity also bounds the amplitude by one.



$H = \varepsilon X$

solid: $|\sin u|$
dashed: $\min(1, u)$

Probability is $\sin^2 u$, not $|\sin u|$.

From a norm to a probability

For this initial state, the escape probability is $\sin^2(\varepsilon t)$, not $|\sin(\varepsilon t)|$. Consequently

$$\Pr(\text{hidden packet at } t) \le \min\{1, \varepsilon^2 t^2\}.$$

At $\varepsilon t = \pi/6$, the amplitude is $1/2$ and the probability is $1/4$. Near zero, amplitudes are first order while escape probabilities are second order. Mixing those two quantities produces an incorrect interpretation of a leakage plot.

The figure displays samples of the explicit functions above. The supporting check verifies the exact exponential identity, its unitarity, the squared leakage matrix, and the special-time value. The paper's theorem supplies the bound for all times within its stated scope.

At larger times amplitude can return from the hidden packet. The commutator bound therefore limits the largest possible leakage without predicting that it must rise monotonically.

> **Read this as:** The norm estimate controls amplitude. For a normalized state, square it to obtain a probability bound, and retain the distinction between a bound and the actual oscillatory dynamics.

V12 / NOT ALL MOTION IS PHYSICAL EVOLUTION

A moving frame creates a connection term

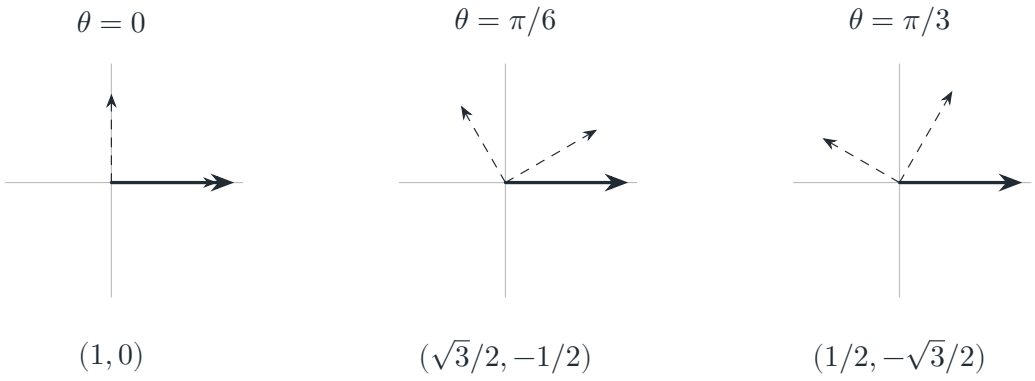
Traditional p. 46 / Theorem II.6.3.

Set the laboratory Hamiltonian to zero and keep $\psi(t) = |0\rangle$ fixed. Describe it in rotating coordinates,

$$U(t) = \begin{pmatrix} \cos t & -\sin t \\ \sin t & \cos t \end{pmatrix}, \qquad y(t) = U(t)^* \psi(t) = \begin{pmatrix} \cos t \\ -\sin t \end{pmatrix}.$$

The vector has not moved in the laboratory, but its coordinate entries have changed.

Solid vector: fixed in the laboratory. Dashed axes: rotating frame.



The missing term can be computed exactly

Let $J = \begin{pmatrix} 0 & -1 \\ 1 & 0 \end{pmatrix}$. Since $U^*\dot{U} = J$, the coordinate Hamiltonian is

$$H_{\text{frame}} = -\mathrm{i}J = \begin{pmatrix} 0 & \mathrm{i} \\ -\mathrm{i} & 0 \end{pmatrix}, \qquad \mathrm{i}\dot{y} = H_{\text{frame}} y.$$

This matrix is Hermitian. Omitting it would predict a constant y, contradicting the displayed coordinates. In this example the norm of the omitted time derivative is exactly one, so the failure is not a small numerical residual.

For a nonzero laboratory Hamiltonian, the same product rule adds the transformed physical term U^*HU. Thus $U^*HU - \mathrm{i}U^*\dot{U}$ separates the physical generator from the coordinate correction. Both pieces belong to the same equation but have different origins.

The drawing shows actual rotated axes at three angles, not three different laboratory trajectories. The check differentiates the exact matrices and verifies the coordinate Schrödinger equation symbolically. The explicit derivatives make a numerical difference approximation unnecessary.

> **Read this as:** When coordinates move, even a stationary physical vector acquires changing components. The connection term accounts for that change without adding a force to the laboratory system.

V13 / THE CANONICAL PACKET CONNECTION

Differentiate the subspace itself

Traditional p. 45 / Theorem II.6.1, Theorem II.6.2.

Continue with $P(t) = U(t)\,\mathrm{diag}(1,0)U(t)^*$ and $Q(t) = I - P(t)$. Differentiating $P^2 = P$ gives

$$\dot{P}P + P\dot{P} = \dot{P}, \qquad P\dot{P}P = 0.$$

The second identity says that the derivative has no component entirely inside the current packet. It moves the subspace relative to its complement.

$P(0)$

1	0
0	0

$\dot{P}(0)$

0	1
1	0

C

0	-1
1	0

$$P\dot{P}P = 0, \qquad C^* = -C, \qquad [C, P] = \dot{P}.$$

For this complete pair of packets, define

$$C = \dot{P}P + \dot{Q}Q.$$

Exact calculation yields the constant matrix $C = J$, with $C^* = -C$ and $[C, P] = \dot{P}$. At $t = 0$, the displayed small matrices allow these identities to be checked by direct multiplication.

From two packets to a complete family

For differentiable orthogonal projectors P_a summing to the identity, the paper constructs

$$C = \sum_a \dot{P}_a P_a = \frac{1}{2}\sum_a [\dot{P}_a, P_a].$$

This single connection reproduces the motion of every packet in the family. No basis within a packet is needed for this formula. A basis choice would add internal coordinate data without changing which subspaces are selected.

The completeness of the family matters in deriving skew-Hermiticity and the simultaneous transport identities. Using only one summand of an incomplete list is not automatically the same connection. The example retains both P and Q throughout, even when the picture emphasizes only the first line.

> **Read this as:** The projector derivative describes motion between subspaces. The canonical connection reconstructs that motion from the complete family without choosing internal packet bases.

V14 / THE RANGE BUNDLE IS CONSTRUCTED LOCALLY

A chart failure is not a singular fiber

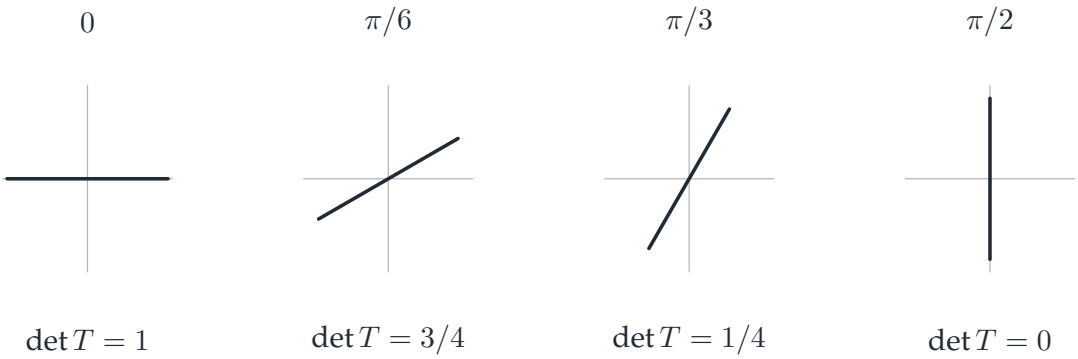
Traditional p. 49 / Theorem II.6.7. Details of the range atlas: saved v0.6.0 supplement, pp. 2–4.

The fiber of a projector field is the actual fixed subspace $E_x = \{v : P(x)v = v\}$. To compare it with a nearby anchor fiber E_a, the completion proof constructs

$$T_a(x) = P(x)P(a) + (I - P(x))(I - P(a)).$$

It equals the identity at the anchor and intertwines the two projectors. Where it is invertible, its restriction provides local fiber coordinates.

The ranges of $P(\theta)$ are shown with a horizontal anchor.



At the last position, use a new anchor. The fiber still has dimension one.

An exact example of the domain restriction

For the rotating line and anchor $P(0)$,

$$T_0(t) = \cos t\, U(t), \qquad \det T_0(t) = \cos^2 t.$$

The chart fails at $t = \pi/2$, but $P(\pi/2) = \operatorname{diag}(0, 1)$ is a perfectly regular rank-one projector. Choosing a vertical anchor supplies a new chart there. What failed was the comparison with one reference fiber, not the fiber itself.

In general, the open sets where $T_a(x)$ is invertible cover the base. The inverse chart maps and smooth overlap maps are constructed from the actual matrices. Their cocycle identities express consistent coordinate changes, rather than assuming a global basis exists.

The v0.6.0 supplement proves the intrinsic connection and its curvature using actual manifold derivatives. Its scope includes bounded idempotents, not only orthogonal ones. The illustration uses a finite-dimensional orthogonal projector to make the construction visible. Those simplifying choices do not restrict the recorded theorem.

> **Read this as:** A smooth bundle is built from compatible local charts. The singularity of one chart determinant can be harmless, provided another anchor covers the same smooth fiber.

V15 / AN EXACT BLOCH PROJECTOR CALCULATION

Curvature measures a local area response

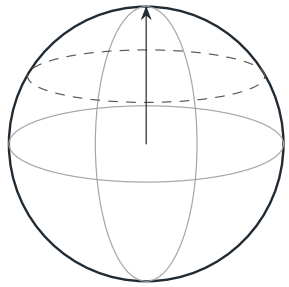
Traditional p. 49 / Theorem II.6.7, Corollary II.6.8.

On the unit sphere, set $n = (\sin\theta\cos\phi, \sin\theta\sin\phi, \cos\theta)$ and

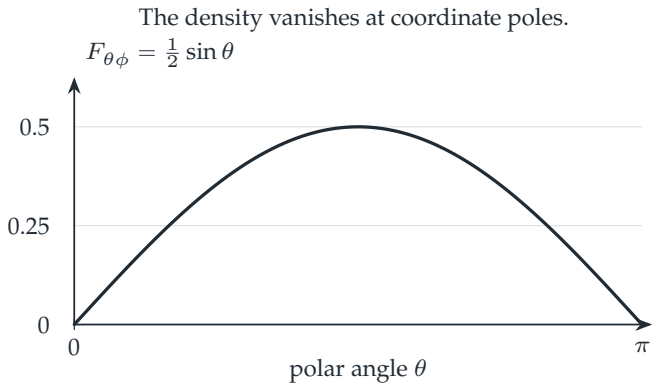
$$P(\theta,\phi) = \frac{1}{2}(I + n\cdot\sigma).$$

This is a smooth rank-one orthogonal projector. The intrinsic curvature is the endomorphism-valued two-form $P(\mathrm{d}P\wedge\mathrm{d}P)P$. With the paper's scalar convention, its component is

$$F_{\theta\phi} = -\mathrm{i}\,\mathrm{Tr}\big(P[\partial_\theta P, \partial_\phi P]\big) = \frac{1}{2}\sin\theta.$$



Cap flux at $\theta = \pi/3$ is $\pi/2$.



A local frame gives the same answer

Away from the south pole, use $u_N = (\cos(\theta/2), e^{\mathrm{i}\phi}\sin(\theta/2))^T$. Then $P = u_N u_N^*$ and the scalar one-form is

$$A_N = -\mathrm{i}u_N^*\mathrm{d}u_N = \frac{1-\cos\theta}{2}\,\mathrm{d}\phi, \qquad \mathrm{d}A_N = \frac{1}{2}\sin\theta\,\mathrm{d}\theta\wedge\mathrm{d}\phi.$$

Thus the curvature flux through the cap $0 \le \theta \le \theta_0$ is $\pi(1-\cos\theta_0)$. At $\theta_0 = \pi/3$, it is exactly $\pi/2$. The latitude drawn in the plate illustrates this cap. The exact flux comes from the formula above.

The vanishing of the coordinate density at a pole does not mean the geometric curvature disappears there. The spherical area form also carries the factor $\sin\theta$. Assigning a phase to parallel transport also requires an orientation and a sign convention for the connection. These choices determine how flux relates to phase.

> **Read this as:** The projector formula and a local frame calculation agree. Curvature is intrinsic even when no single smooth frame covers the whole sphere.

V16 / THE ANSWER DEPENDS ON ITS EFFECTS

Which coherence can a measurement see?

Traditional pp. 50, 51 / Theorem II.7.2, Theorem II.7.4, Corollary II.7.5.

For the Bell density matrix $\rho = |\Phi^+\rangle\langle\Phi^+|$, parity dephasing does nothing: both nonzero amplitudes already lie in the even subspace. Dephasing in the computational basis removes the entries between addresses 00 and 11.

2ρ, also $2D_{\text{parity}}(\rho)$

00	1	0	0	1
01	0	0	0	0
10	0	0	0	0
11	1	0	0	1

same diagonal
different coherence

$2D_{\text{computational}}(\rho)$

00	1	0	0	0
01	0	0	0	0
10	0	0	0	0
11	0	0	0	1

Bell-projector outcome: 1 on the left, $1/2$ on the right.

Every effect in the computational basis $E_a = |a\rangle\langle a|$ has the same expectation on both matrices, namely $1/2$ at 00 and 11 and zero elsewhere. These measurements read only the diagonal. They cannot distinguish the pure Bell state from this incoherent mixture.

A measurement that resolves the difference

Use the valid two-outcome measurement with effects $E = \rho$ and $I - E$. Then

$$\operatorname{Tr}(E\rho) = 1, \qquad \operatorname{Tr}\big(ED_{\text{computational}}(\rho)\big) = \frac{1}{2}.$$

The effect itself is not diagonal in the fine computational packets. It compares their coherent combination, so it falls outside the paper's invariance result for block-diagonal effects.

This example contains three operations that should not be conflated: representing a state by all of its packet matrix blocks, applying a dephasing channel, and reading one specified measurement. Only the second discards the off-diagonal blocks. The third may or may not notice that loss, depending on its effects.

The exact checks construct all four fine projectors, both parity projectors, both dephased states, and the outcome traces. They reject the stronger statement that *every* measurement is invariant under dephasing.

> **Read this as:** A measurement's inability to see a coherence does not make that coherence absent. It states a restriction on the observable, not an equality of the underlying states.

V17 / POPULATIONS AND COHERENCES TRANSFORM DIFFERENTLY

A channel acts on four matrix entries

Traditional pp. 52, 54 / Theorem II.7.6, Example II.7.12.

Choose amplitude damping with $\gamma = 9/25$:

$$K_0 = \begin{pmatrix} 1 & 0 \\ 0 & 4/5 \end{pmatrix}, \qquad K_1 = \begin{pmatrix} 0 & 3/5 \\ 0 & 0 \end{pmatrix}, \qquad K_0^* K_0 + K_1^* K_1 = I.$$

The channel $\Phi(\rho) = \sum_a K_a \rho K_a^*$ is trace preserving and completely positive. The special parameter keeps every displayed coefficient rational.

Superoperator on matrix entries

	00	01	10	11
00	1	0	0	$\frac{9}{25}$
01	0	$\frac{4}{5}$	0	0
10	0	0	$\frac{4}{5}$	0
11	0	0	0	$\frac{16}{25}$

$\gamma = 9/25$

coherence factor $4/5$

Output from $|+\rangle$

$\frac{17}{25}$	$\frac{2}{5}$
$\frac{2}{5}$	$\frac{8}{25}$

$$\operatorname{Tr}\rho = 1, \quad \det\rho = 36/625 > 0$$

The superoperator uses the entry order $(\rho_{00}, \rho_{01}, \rho_{10}, \rho_{11})$. Population leaves the excited state with factor $9/25$, while coherences contract by $4/5$. These are not the same rate or the same coordinate.

For $\rho_+ = \frac{1}{2}\begin{pmatrix} 1 & 1 \\ 1 & 1 \end{pmatrix}$, the exact output is

$$\Phi(\rho_+) = \begin{pmatrix} 17/25 & 2/5 \\ 2/5 & 8/25 \end{pmatrix}.$$

Its trace is one and determinant is $36/625 > 0$, so it is a mixed positive state. Arrows that show population transfer alone would leave its off-diagonal entries unspecified.

How complete positivity is certified

The Choi matrix is an explicit sum of two outer products of vectorized Kraus operators. Its eigenvalues are $41/25, 9/25, 0, 0$, all nonnegative. This gives an independent finite certificate in addition to Kraus normalization. The Choi matrix has trace two under the convention used by the check, which leaves the maximally entangled vector unnormalized.

> **Read this as:** A packet channel acts on pairs of packet addresses, because density matrices have two indices. Population transfer alone does not reconstruct a quantum channel.

V18 / WHY COMPLETE POSITIVITY IS THE RELEVANT CONDITION

An ancilla tests more than positivity

Traditional p. 52 / Classical input II.7.7.

Ordinary transpose T sends a positive matrix on one system to another positive matrix and preserves its trace. Those properties are insufficient for a quantum channel on a subsystem of an entangled state. The test must include id ⊗T on the larger system.

$2(\mathrm{id}\otimes\mathsf{T})(\rho_{\mathrm{Bell}})$

00	1	0	0	0
01	0	0	1	0
10	0	1	0	0
11	0	0	0	1

$$w = (|01\rangle - |10\rangle)/\sqrt{2}$$

$$w^*(\mathrm{id}\otimes\mathsf{T})(\rho)w = -1/2$$

Transpose is positive on one system.
It is not completely positive.

Apply this extended map to the Bell density matrix. The result is

$$(\mathrm{id}\otimes\mathsf{T})(\rho_{\mathrm{Bell}}) = \frac{1}{2}\begin{pmatrix}1&0&0&0\\0&0&1&0\\0&1&0&0\\0&0&0&1\end{pmatrix}.$$

Its middle block has one negative eigenvalue. More concretely, the normalized vector $w = (|01\rangle - |10\rangle)/\sqrt{2}$ satisfies

$$w^*(\mathrm{id}\otimes\mathsf{T})(\rho_{\mathrm{Bell}})w = -\frac{1}{2}.$$

This exact negative value of the quadratic form certifies failure of positivity on the composite system. No numerical eigenvalue tolerance is needed.

Why the Kraus form avoids this problem

For every auxiliary dimension and positive X, each term $(I \otimes K_a)X(I \otimes K_a)^*$ is positive. Their sum is positive as well. This argument explains the word *completely*. The conclusion holds for every auxiliary dimension, which a test of one input density matrix on the original system cannot establish.

The transpose counterexample is an explanatory finite calculation, not a new addition to the formal theorem count. It makes visible the hypothesis that the manuscript's Kraus result already supplies. The exact check constructs the partial transpose with the stated tensor indexing and evaluates its negative witness directly.

> **Read this as:** A map can look harmless on an isolated system and fail on an entangled extension. Complete positivity retains compatibility with every auxiliary system.

V19 / FOUR EXACT SYNDROME PACKETS

Find the error without reading the logical state

Traditional pp. 56, 57, 59 / Theorem II.8.2, Theorem II.8.4, Example II.8.8.

Encode a qubit by $|0_L\rangle = |000\rangle$ and $|1_L\rangle = |111\rangle$. Let P project onto this code and take errors $E_a \in \{I, X_1, X_2, X_3\}$. Their images are four orthogonal rank-two packets $Q_a = E_a P E_a^*$ that sum to the full identity.

Channel probabilities: $1/10,\ 2/10,\ 3/10,\ 4/10$.

no error	X_1	X_2	X_3
$\|000\rangle$	$\|100\rangle$	$\|010\rangle$	$\|001\rangle$
$\|111\rangle$	$\|011\rangle$	$\|101\rangle$	$\|110\rangle$
ratio $3:4$	ratio $3:4$	ratio $3:4$	ratio $3:4$

Use the logical state $\psi = (3|0_L\rangle + 4|1_L\rangle)/5$ and channel probabilities $w = (1, 2, 3, 4)/10$. The noisy state is $\sum_a w_a E_a \psi\psi^* E_a^*$. A syndrome measurement returns label a with probability w_a, independent of the logical amplitudes.

The recovery is an actual channel

The operators $R_a = E_a^* Q_a$ satisfy $\sum_a R_a^* R_a = I$. Applying the recovery $\mathcal{R}(X) = \sum_a R_a X R_a^*$ to the noisy state gives exactly $\psi\psi^*$. The off-diagonal logical coherence $12/25$ is recovered as well as the populations $9/25$ and $16/25$.

The Knill–Laflamme compressions are $P E_a^* E_b P = \delta_{ab} P$. Their scalar form says that the error labels do not resolve the encoded vector. The exact checks evaluate all sixteen compressions, all sixteen syndrome products, the four probabilities, the recovery normalization, and the full recovered matrix.

This code corrects the specified flips of individual bits. That result does not cover arbitrary errors on three qubits or arbitrary errors on a single qubit. The next example exhibits an error outside its protected family.

> **Read this as:** A syndrome identifies an error subspace while leaving a two-dimensional logical subspace intact. Measuring the two logical basis states separately would destroy the information the recovery must preserve.

V20 / THE SCALAR COMPRESSION TEST MATTERS

An unchanged syndrome can hide a logical error

Traditional pp. 56, 58 / Theorem II.8.2, Proposition II.8.7.

Apply $Z_1 = Z \otimes I \otimes I$ to the same repetition code. It sends $|000\rangle$ to itself and $|111\rangle$ to its negative. Both states remain inside the original code, so the previous syndrome partition reports no bit flip.

$$\frac{3|000\rangle + 4|111\rangle}{5} \longmapsto \frac{3|000\rangle - 4|111\rangle}{5}.$$

The populations are unchanged, but the relative phase is not.

$V^* Z_1 V$

1	0
0	-1

before: $(3, 4)/5$

after: $(3, -4)/5$

same code support
different relative phase

Required scalar form cI

c	0
0	c

A trace of zero does not make $\mathrm{diag}(1, -1)$ the zero operator.

Let V be the code isometry with columns $|000\rangle, |111\rangle$. For the proposed error family $\{I, Z_1\}$, its off-diagonal error compression is

$$V^* I^* Z_1 V = \begin{pmatrix} 1 & 0 \\ 0 & -1 \end{pmatrix}.$$

This matrix is not cI for any scalar c. Thus the Knill–Laflamme condition fails for that family. Its trace is zero even though its action on the code is nonzero. A trace test alone would miss the obstruction.

Known correction versus family recovery

If it is known with certainty that Z_1 occurred, applying Z_1 again reverses it. The failed criterion concerns a *single recovery valid for every unknown error in the declared family*, not invertibility of each error considered separately. This distinction prevents a misleading conclusion that no phase error can ever be undone.

The finite calculation checks the actual compressed matrix and rejects its equality to zero. The scalar obstruction is then transparent from the two unequal diagonal entries.

> **Read this as:** Correction must preserve all logical superpositions for the declared error family. Staying in the code and preserving basis probabilities are not sufficient.

V21 / TWO INVERTIBILITY CONDITIONS, NOT ONE

Hidden states return as spectral dependence

Traditional p. 60 / Theorem II.9.2, Theorem II.9.3.

Take $H = \begin{pmatrix} 0 & 1 \\ 1 & 2 \end{pmatrix}$ and retain its first coordinate. The eliminated block is $H_{QQ} = 2$. Whenever $z-2$ and the full $zI - H$ are invertible,

$$H_{\text{eff}}(z) = \frac{1}{z-2}, \qquad [(zI-H)^{-1}]_{00} = \frac{1}{z - 1/(z-2)} = \frac{z-2}{z^2-2z-1}.$$

This is the corrected hypothesis set recorded in the formal release.

Filled: full resolvent poles. Open at 2: only the eliminated inverse fails.



At $z = 3$: exact retained resolvent $1/2$, bare truncation $1/3$.

At $z = 3$, the exact retained resolvent is $1/2$. Bare truncation uses only $H_{PP} = 0$ and gives $1/3$, an error of $1/6$. The omitted coupling has changed the response even though the retained diagonal entry did not change.

A pole can belong to the elimination chart

At $z = 2$, the eliminated inverse does not exist, so the displayed Schur formula cannot be applied there as written. Nevertheless, the full resolvent exists and its retained entry is zero. The rational expression has a continuation to this value. By contrast, $1 \pm \sqrt{2}$ are poles of the full resolvent.

Invertibility of the full matrix is an independent requirement. At $z = 0$, $H = \operatorname{diag}(0, -1)$ has an invertible eliminated block in $zI - H$, but the full matrix is singular. The original prose omitted this condition. The preserved amendments restore it. This appendix uses the corrected form throughout.

> **Read this as:** An exact elimination formula has a spectral domain. Check both inverses before evaluating it, and distinguish poles of an intermediate inverse from poles of the full physical resolvent.

V22 / AN EXACT QUANTUM MEMORY EQUATION

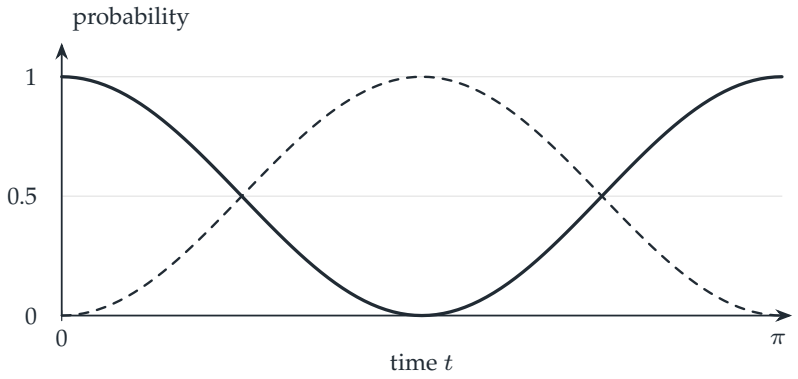
The smaller system remembers the discarded one

Traditional pp. 63, 64 / Theorem II.9.8, Theorem II.9.11.

Choose $H = X$, initial state $(1, 0)^T$, and retain the first coordinate. The coupled equations and their solution are

$$\mathrm{i}\dot{x} = y, \qquad \mathrm{i}\dot{y} = x, \qquad x(t) = \cos t, \quad y(t) = -\mathrm{i}\sin t.$$

The hidden probability returns periodically. Deleting the hidden row and column would instead leave the zero Hamiltonian and predict $x(t) = 1$.



solid: retained
dashed: hidden

$K(t) = 1$

The two probabilities sum to one.

Eliminate exactly, not approximately

Integrating the second equation with $y(0) = 0$ gives $y(t) = -\mathrm{i}\int_0^t x(s)\,ds$. Substitution produces

$$\dot{x}(t) = -\int_0^t x(s)\,ds.$$

The memory kernel is the constant function one. Differentiating once more recovers $\ddot{x} = -x$ with $x(0) = 1$ and $\dot{x}(0) = 0$, explaining the cosine solution. A nonzero hidden initial state would add a forcing term that must also be retained.

The full propagator is a unitary group, but its retained scalar entry is not a semigroup. At $t = s = \pi/4$,

$$x(t + s) - x(t)x(s) = 0 - \frac{1}{2} = -\frac{1}{2}.$$

There is no contradiction: compression of a product need not equal the product of the compressed factors when the hidden subspace carries intermediate amplitude.

The check verifies the differential and integral equations symbolically and the displayed nonzero semigroup defect exactly. The curves visualize the explicit solution and its periodic return of amplitude.

> **Read this as:** Exact elimination replaces a hidden coordinate with memory and forcing from the initial data. Replacing that memory by a constant generator is an additional approximation, not part of the exact theorem.

V23 / SPECTRAL POSITIVITY IS BASIS INDEPENDENT

Positive transfer is not a stochastic matrix

Traditional p. 66 / Theorem II.10.1, Theorem II.10.3.

For $H = I - X$, the two eigenvalues are zero and two. Its Euclidean transfer is

$$T(\tau) = e^{-\tau H} = \frac{1}{2}\begin{pmatrix} 1+q & 1-q \\ 1-q & 1+q \end{pmatrix}, \qquad q = e^{-2\tau}.$$

For $\tau \geq 0$, the eigenvalues $1, q$ lie in $(0, 1]$, and multiplying two such matrices replaces q, r by qr. This is the semigroup law in spectral coordinates.

T at $e^{-2\tau} = 1/2$

$\frac{3}{4}$	$\frac{1}{4}$
$\frac{1}{4}$	$\frac{3}{4}$

Both have spectrum $\{1, 1/2\}$.

ZTZ in another basis

$\frac{3}{4}$	$-\frac{1}{4}$
$-\frac{1}{4}$	$\frac{3}{4}$

Positive-definite operator: $v^* T v > 0$ for $v \neq 0$. Not an entrywise test.

At $q = 1/2$, the displayed T happens also to have nonnegative entries and column sums one. Conjugate by the unitary Z. The spectrum and positivity of the quadratic form are preserved, but both off-diagonal entries become $-1/4$. Thus positivity as an operator is not entrywise positivity and does not by itself give a Markov interpretation.

A useful finite positive kernel

For this nonnegative H, vectors u_a and times $t_a \geq 0$ satisfy

$$\sum_{a,b} \langle u_a, e^{-(t_a+t_b)H} u_b \rangle = \left\| \sum_a e^{-t_a H} u_a \right\|^2 \geq 0.$$

The factorization makes positivity transparent. It remains a finite operator identity. A continuum reconstruction theorem requires a compatible field structure, limits, positivity hypotheses, and the other assumptions of the chosen reconstruction framework. Each of these assumptions requires its own justification beyond the two positive eigenvalues.

The exact check verifies the matrix semigroup law as a polynomial identity in q, r and verifies the unchanged spectrum after conjugation. It rejects entrywise nonnegativity for the conjugated matrix.

> **Read this as:** Euclidean positivity refers to quadratic forms and spectral values. A stochastic interpretation or a continuum physical reconstruction needs additional structure.

V24 / THE EXACT HEAT TRACE ON FOUR SITES

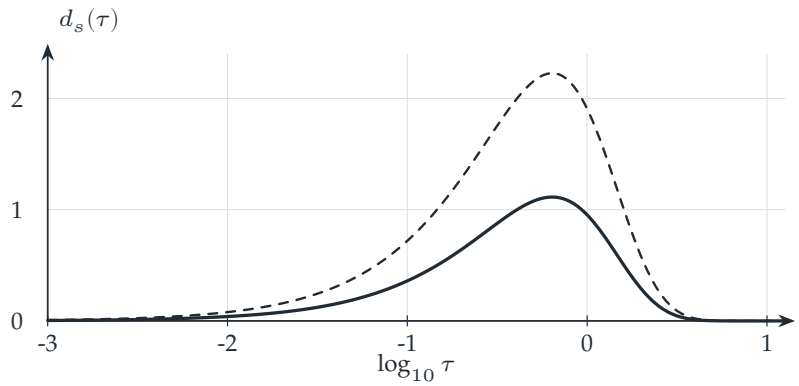
A dimension curve is a scale diagnostic

Traditional p. 68 / Definition II.11.1, Proposition II.11.2.

For the Laplacian on a cycle with four sites $L = 2I - S - S^*$, the eigenvalues are $0, 2, 2, 4$. The normalized heat trace and its diagnostic of spectral dimension are therefore

$$K(\tau) = \frac{1 + 2e^{-2\tau} + e^{-4\tau}}{4} = \frac{(1 + e^{-2\tau})^2}{4}, \qquad d_s(\tau) = -2\tau \frac{K'(\tau)}{K(\tau)} = \frac{8\tau}{e^{2\tau} + 1}.$$

No numerical differentiation is needed for this finite example.



solid: four-cycle
dashed: product of two

No broad plateau is promised at four sites.

Finite diagnostic, not a dimension proof.

Both ends reflect the finite size of the system

As $\tau \to 0$, every eigenmode contributes approximately one and the dimension diagnostic tends to zero. As $\tau \to \infty$, the zero mode dominates, so it again tends to zero. A finite spectrum cannot sustain a nonzero plateau at all scales.

For the Cartesian product of two identical cycles with four sites, the Laplacian eigenvalues add and the heat traces multiply: $K_2 = K^2$. Consequently $d_{s,2} = 2d_s$ exactly. The product identity determines the second curve exactly from the first.

At $\tau = \log 2/2$, the first curve equals $4 \log 2/3$. This noninteger value is a spectral quantity that depends on scale, not a claim that the graph has a fractional topological dimension. Four sites are too few to promise a broad geometric plateau. Experiments on larger grids remain finite diagnostics. Convergence requires the analytic hypotheses developed on V37.

> **Read this as:** A convincing continuum dimension needs a stable scale window that persists under controlled refinement. One appealing finite curve is not that theorem.

V25 / AN EXACT ERROR ENCLOSURE, NOT A FITTED SLOPE

Refine the grid while holding the mode fixed

Traditional p. 69 / Theorem II.11.4.

For the circle symbol, the continuum value is k^2 and the grid value is

$$\lambda_{k,h} = \frac{4}{h^2}\sin^2\left(\frac{kh}{2}\right), \qquad h \neq 0.$$

For a fixed low mode, the paper bounds the error by $0 \leq k^2 - \lambda_{k,h} \leq k^4 h^2/12$. The spacing condition matters because the displayed expression divides by h^2.

$h = \frac{1}{4}$	$h = \frac{1}{8}$	$h = \frac{1}{16}$
error (approx.)	error (approx.)	error (approx.)
$\simeq 0.005197495$	$\simeq 0.001301405$	$\simeq 0.000325478$
bound $h^2/12$	bound $h^2/12$	bound $h^2/12$
$\frac{1}{192}$	$\frac{1}{768}$	$\frac{1}{3072}$

Successive error ratios lie strictly between 3.99 and 4.

What is certified in the displayed table?

Take $k = 1$ and $h = 1/4, 1/8, 1/16$. For $x = h/2 \in [0, 1]$, alternating Taylor sums give rational lower and upper bounds for $\sin x$. Squaring these positive endpoints and multiplying by $4/h^2$ yields exact rational enclosures for each error. The displayed decimals only locate those much narrower rational intervals.

Each interval lies strictly inside $(0, h^2/12)$. Dividing successive interval endpoints proves that both error ratios are between 3.99 and 4. The check verifies these inequalities by rational arithmetic, without relying on approximate sine values or a fitted logarithmic slope.

Why the mode regime matters

If instead $k = \pi/h$ moves with the grid, the ratio $\lambda_{k,h}/k^2 = 4/\pi^2$ stays constant, not one. The bound's factor k^4 warns that it is not uniform in arbitrary moving high modes. The displayed rational test evaluates the analytic symbol. It does not assert that every chosen spacing defines an integer periodic grid.

> **Read this as:** Second-order convergence is a quantified statement with a specified mode regime. Keep that regime fixed when reading an error curve or comparing refinements.

V26 / TEST THE CONSTRAINTS BEFORE THE PROJECTION

A zero compressed anomaly can be automatic

Traditional pp. 71, 72 / Theorem II.12.2, Proposition II.12.3.

Take the self-adjoint matrices

$$C_1 = \operatorname{diag}(0, 1, -1), \qquad C_2 = \begin{pmatrix} 0 & 0 & 0 \\ 0 & 0 & 1 \\ 0 & 1 & 0 \end{pmatrix}, \qquad P = \operatorname{diag}(1, 0, 0).$$

Both constraints annihilate $P\mathbb{C}^3$, and their common kernel is exactly that one-dimensional space. Nevertheless, their full commutator is nonzero.

$[C_1, C_2]$

0	0	0
0	0	2
0	−2	0

$P = \operatorname{diag}(1, 0, 0)$

$C_1 P = C_2 P = 0$

$P[C_1, C_2]P$

0	0	0
0	0	0
0	0	0

The right matrix is zero by the common-kernel choice, not by operator closure.

Why the compressed test cannot decide closure

Since $C_1 P = C_2 P = 0$, each product $C_1 C_2 P$ and $C_2 C_1 P$ vanishes. Therefore $P[C_1, C_2]P = 0$ without any requirement that the unprojected commutator close in the chosen constraint span. In this example the skew off-diagonal commutator is not a linear combination of the two displayed symmetric constraints.

More generally, an anomaly expression made from their commutators and linear combinations of constraints also kills an exact projector onto the common kernel on the right. The formal release records this limit of the diagnostic. A nonzero compressed residual can reveal inconsistent proposed data, but an automatic zero does not construct an anomaly-free constraint algebra.

A substantive closure analysis must inspect the operator relations, their domains, the actual physical subspace, and compatibility under refinement. For infinite systems, these questions also involve domain and limit control that finite matrix arithmetic cannot replace.

The exact example computes both constraint products, the full commutator, and its compression. It deliberately rejects the inference from compressed zero to unprojected zero.

> **Read this as:** Before interpreting a vanishing residual, check whether the definition of its projector already forces it to vanish. A tautological diagnostic cannot supply the missing existence or closure theorem.

V27 / SEEDS, CHARACTERS, INTERFERENCE, AND DEPHASING

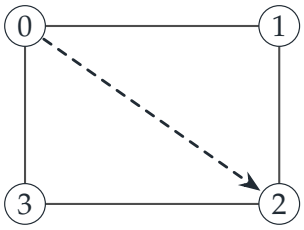
One calculation of transfer to the opposite site

Traditional pp. 39, 42, 50 / Corollary II.3.3, Theorem II.4.4, Theorem II.7.4.

Return to the shift on four sites S and Laplacian $L = 2I - S - S^*$. The same character projectors have energies $(0, 2, 4, 2)$. At time $t = \pi/2$, their evolution phases are $(1, -1, 1, -1)$, exactly the character eigenvalues of S^2. Hence

$$e^{-\mathrm{i}\pi L/2} = S^2, \qquad |0\rangle \longmapsto |2\rangle.$$

$e^{-\mathrm{i}\pi L/2} = S^2$



start	time $\pi/2$
1	0
0	0
0	1
0	0

Target probability after partial momentum dephasing: $1 - 3\eta/4$.

At halfway time $\pi/4$, the actual amplitude vector is $(-\mathrm{i}, 1, \mathrm{i}, 1)^T/2$, giving uniform site probabilities. The subsequent phases recombine those four amplitudes into a single output at the opposite site. Uniform intermediate probabilities do not imply an incoherent intermediate state.

A channel changes the conclusion predictably

Before evolving, mix the seed density matrix with its complete momentum dephasing:

$$\rho_\eta = (1-\eta)|0\rangle\langle 0| + \eta \sum_j P_j |0\rangle\langle 0| P_j = (1-\eta)|0\rangle\langle 0| + \eta I/4, \quad 0 \le \eta \le 1.$$

At transfer time, the probability at the opposite site is exactly $1 - 3\eta/4$. Complete momentum dephasing reduces it to $1/4$. This calculation isolates how discarded coherence changes the interference result.

Finally, the shift grammar generates four independent vectors from $|0\rangle$, while the Hamiltonian powers generate only three: its repeated energy links two momentum directions. The same seed can therefore be cyclic for the shift algebra and noncyclic for the Hamiltonian algebra, even though perfect transfer occurs at one time.

> **Read this as:** Perfect transfer is an exact finite interference statement. It neither implies cyclicity for every operator grammar nor survives an unaccounted dephasing operation.

V28 / AN EVIDENCE GUIDE FOR THE READER

What these pictures establish

Traditional p. 78 / Section II.14. Saved formal scope: v0.6.0 ledger and completion supplement.

The appendix uses small objects to make the paper's constructions inspectable. Every matrix and finite example is supplied in editable source, with a separate check record. The plates make those calculations visible. Their appearance helps explain the result, while the equations and check records supply its evidence.

Evidence	What it supports	What it does not supply
Exact matrices	The displayed finite identities, witnesses, and counterexamples.	A classification of arbitrary systems.
Symbolic derivatives	The explicit rotating and Bloch examples.	A proof inferred from numerical differentiation.
Rational enclosures	The three displayed dispersion intervals and ratio inequalities.	A continuum theorem from three sample points.
Saved Lean release	Its 19 registered finite items under their recorded hypotheses.	A fresh kernel run for this appendix.
Numerical record	The original finite software examples in the tested environment.	Physical experiments or unrestricted convergence.

Which source is authoritative?

The saved formal checkpoint is v0.6.0: 323 recorded theorem declarations in 25 current modules, including supporting lemmas. These counts describe the inherited checkpoint. This prose revision includes no new Lean kernel execution. The final traditional edition supplies the current reading references. The original proof sources and the separate v0.5.1 editorial sibling retain their own identities.

The five research boundaries remain separate: an anomaly-free coherent refinement, uniform control of effective operators, Lorentzian reconstruction, an Einstein infrared limit, and a positive physical massless spin-two sector. A finite projector bundle, positive transfer matrix, or spectral diagnostic does not settle them.

A practical way to use the appendix

Choose one page, reproduce its matrix calculation, and then read the cited theorem with its hypotheses. The retained execution records give the exact assertions, tested ranges, and rejected controls for the finite and symbolic suites. The additional examples and their recorded bounds are described on V40. In particular, retain the two resolvent assumptions on V21, the distinction between a known error and an error family on V20, and the limitation of testing only the common kernel on V26.

> **Read this as:** Exact finite structure is valuable because its boundary is explicit. The appendix adds understanding and reproducibility, not unproved continuum claims or a new theorem count.

V29 / A SIX-DIMENSIONAL REGULAR REPRESENTATION

Nonabelian packets carry multiplicity

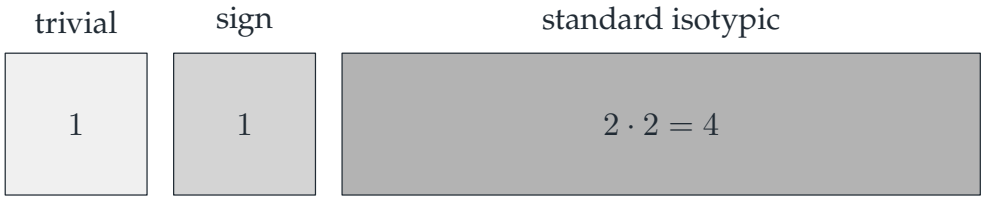
Traditional p. 38 / Theorem II.3.1, Theorem II.3.2.

Let $\mathcal{H} = \mathbb{C}[S_3]$ have the six orthonormal basis vectors $|g\rangle$, with left action $U(h)|g\rangle = |hg\rangle$. The irreducible characters on the identity, transposition, and three-cycle classes are

	e	(12)	(123)	d_λ
trivial	1	1	1	1
sign	1	-1	1	1
standard	2	0	-1	2

$$P_\lambda = \frac{d_\lambda}{6} \sum_{g \in S_3} \chi_\lambda(g^{-1}) U(g).$$

All matrices in this example are rational. Multiplying them gives self-adjoint idempotents of ranks $1, 1, 4$, with pairwise zero products and sum I_6.



$$\mathbb{C}[S_3] \cong \mathbb{C} \oplus \mathbb{C} \oplus (\mathbb{C}^2 \otimes \mathbb{C}^2)$$

The standard packet has dimension four

The standard representation occurs twice in the regular representation. Its isotypic component therefore has dimension $2 \cdot 2 = 4$: one factor carries the two-dimensional irreducible action and the other records multiplicity. A character projector selects the whole isotypic component. It does not select a particular copy or a particular internal vector.

Representation matrix units refine the irreducible factor, while leaving the multiplicity factor untouched. Their multiplication law is stronger information than a list of packet ranks. A basis chosen inside this packet supplies coordinates. It does not canonically distinguish the two copies of the standard representation.

What the retained check establishes

The retained exact check constructs all six permutation matrices, tests all 36 multiplication relations, computes the character averages, and checks ranks independently by Gaussian elimination and traces. It rejects the claim that the standard isotypic projector has rank two. This is one specified representation of S_3, not a computational classification of all finite group representations.

> **Read this as:** For a nonabelian symmetry, distinguish irreducible dimension from multiplicity. A central character projector retains both.

V30 / AN EXACT LOCAL CHART AND ITS FAILURE

Rotate whole packets by a polar factor

Traditional p. 47 / Theorem II.6.5, Theorem II.6.6.

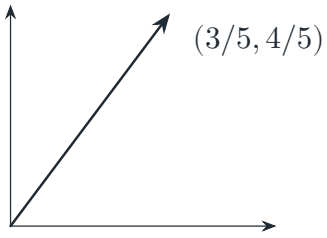
On $\mathcal{H} = \mathbb{C}^2$, put $P_0 = \operatorname{diag}(1,0)$, $P_1 = I - P_0$, and

$$R = \begin{pmatrix} 3/5 & -4/5 \\ 4/5 & 3/5 \end{pmatrix}, \qquad Q_a = RP_aR^*, \qquad S = \sum_{a=0}^{1} Q_aP_a = \frac{3}{5}R.$$

The exact Gram matrices give

$$(S-I)^*(S-I) = \frac{16}{25}I, \quad S^*S = \frac{9}{25}I, \quad \|S-I\| = \frac{4}{5} < 1.$$

Consequently the unitary polar factor is $S(S^*S)^{-1/2} = R$, and $Q_aR = RP_a$ for both complete packets.



$$S = (3/5)R$$
$$S^*S = (9/25)I$$
$$\downarrow$$
$$S(S^*S)^{-1/2} = R$$

The norm condition selects a chart

If the target rank-one packet is orthogonal to the initial one, the two labels are exchanged and $S = 0$. Its polar inverse square root is undefined. This is a failure of this direct local construction, although a unitary carrying one packet system to the other still exists. The strict norm assumption is sufficient, not a global existence criterion for all packet rotations.

Short steps can be composed before reaching a distant endpoint. For example, the rational step $R_1 = \begin{pmatrix} 4/5 & -3/5 \\ 3/5 & 4/5 \end{pmatrix}$ obeys

$$R_1^2 = \begin{pmatrix} 7/25 & -24/25 \\ 24/25 & 7/25 \end{pmatrix}.$$

The multiplication is exact and each step has a valid local overlap. The convergence theorem has a separate analytic contract: a twice continuously differentiable complete projector path on a compact time interval, sufficiently fine partitions, and a constant depending on the path in an $O(|\pi|)$ estimate in operator norm.

Evidence boundary

The retained run checks the Gram identities, polar factor, intertwining, and product of two rational steps. It also checks that the overlap has rank zero when the endpoint packets are orthogonal. It does not certify the analytic convergence theorem by sampling a path.

> **Read this as:** A local polar chart can fail while the subspaces remain regular. Use the stated chart hypothesis and the separate convergence theorem when composing small rotations.

V31 / CHANNEL, CHOI, AND GENERATOR CHECKS

Coherence order survives a covariant channel

Traditional pp. 53, 55 / Theorem II.7.8, Theorem II.7.10, Theorem II.7.14.

Take $S = Z = \mathrm{diag}(1, -1)$ on $\mathbb{C}^2$. Under conjugation $X \mapsto ZXZ$, diagonal matrices have coherence order zero and off-diagonal matrices have coherence order one modulo two. Its projectors on Hilbert–Schmidt operator space are $\mathcal{L}_0(X) = (X + ZXZ)/2$ and $\mathcal{L}_1(X) = (X - ZXZ)/2$.

Choose amplitude damping with $K_0 = \mathrm{diag}(1, 4/5)$ and $K_1 = (3/5)|0\rangle\langle 1|$. The channel is trace preserving, population flows from state one to state zero, and each coherence contracts by $4/5$.

even Choi addresses $00, 11$

$$\begin{pmatrix} 1 & 4/5 \\ 4/5 & 16/25 \end{pmatrix}$$

odd Choi addresses $01, 10$

$$\mathrm{diag}(9/25, 0)$$

$$\Phi(|0\rangle\langle 1|) = (4/5)|0\rangle\langle 1|$$

With the unnormalized Choi convention $J = \sum_{a,b} \Phi(|a\rangle\langle b|) \otimes |a\rangle\langle b|$ and basis $(00, 01, 10, 11)$, the exact matrix is

$$J = \begin{pmatrix} 1 & 0 & 0 & 4/5 \\ 0 & 9/25 & 0 & 0 \\ 0 & 0 & 0 & 0 \\ 4/5 & 0 & 0 & 16/25 \end{pmatrix}, \qquad [J, Z \otimes Z] = 0.$$

The $00, 11$ block is positive and has rank one. The other nonzero eigenvalue is $9/25$. The retained check also verifies that every principal minor is nonnegative.

Symmetry in continuous time has its own hypotheses

For the Lindblad generator with Hamiltonian $H = \mathrm{diag}(0, 2)$ and jump $L = (3/5)|0\rangle\langle 1|$, H has charge zero and L has charge one. Each matrix unit stays within its coherence order under the generator. Replacing H by X breaks that conclusion: the generator then sends a diagonal matrix to off-diagonal entries.

All four input matrix units are checked exactly for channel covariance, generator order preservation, and zero generator trace. The paper uses the finite exponential series to extend generator invariance to the semigroup. The retained calculation uses no numerical solver for the master equation. Symmetry alone does not close the scalar population equations inside packets of higher rank.

> **Read this as:** Charge is a property of operator space. Covariance preserves its coherent sectors, while complete positivity is checked separately through Kraus or Choi data.

V32 / A TOTAL CHANNEL FROM SINGULAR ERROR DATA

Null Gram directions are removed before recovery

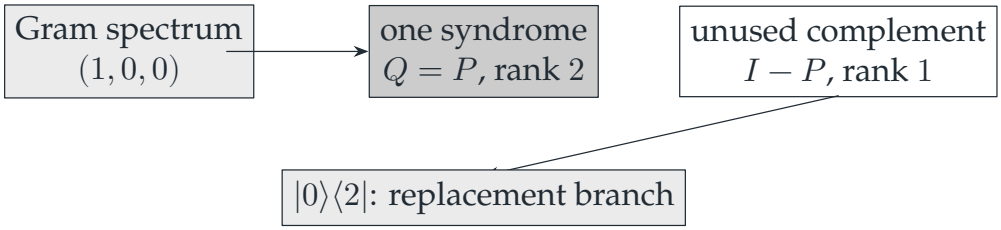
Traditional p. 57 / Theorem II.8.3, Theorem II.8.4.

Let $\mathcal{H} = \mathbb{C}^3$, with nonzero code projector $P = \mathrm{diag}(1, 1, 0)$. On the code use the error family $E_1 = (3/5)P$, $E_2 = (4/5)P$, and $E_3 = 0$. Its Knill–Laflamme Gram matrix is

$$c = \frac{1}{25}\begin{pmatrix} 9 & 12 & 0 \\ 12 & 16 & 0 \\ 0 & 0 & 0 \end{pmatrix}, \qquad PE_a^* E_b P = c_{ab} P.$$

The errors are redundant rather than three distinct syndromes. A real unitary change of error coordinates gives

$$W = \begin{pmatrix} 3/5 & 4/5 & 0 \\ -4/5 & 3/5 & 0 \\ 0 & 0 & 1 \end{pmatrix}, \quad WcW^* = \mathrm{diag}(1, 0, 0), \quad (F_1, F_2, F_3) = (P, 0, 0).$$



Normalize only positive eigenvalues

The positive branch has $V_1 = P$ as an isometry *on the code*, and syndrome support $Q = P$. No factor $\lambda^{-1/2}$ is formed on either zero branch: those branches vanish on the code. Treating them as extra recoverable packets would divide by zero.

The syndrome support is smaller than the ambient space. Define a total recovery with Kraus operators

$$R_1 = P, \qquad R_2 = |0\rangle\langle 2|, \qquad R_1^* R_1 + R_2^* R_2 = I_3.$$

It acts as the identity on operators supported on the code and sends the unused complement population into a chosen code state. The declared error map preserves the trace of code states, so recovery returns every code matrix unit, including both off-diagonal units, exactly. It need not preserve states on the unused complement.

Exceptional cases and scope

This construction assumes a nonzero code so that a complement replacement state exists. The case of a zero code is vacuous and has its own formal statement in the saved ledger. The retained exact run verifies all nine Gram compressions, the diagonalization, both null branches, total channel normalization, and all four code matrix units. It adds no Lean coverage and does not implement a numerical spectral decoder for arbitrary Gram data.

> **Read this as:** Positive Gram support defines genuine syndrome isometries. Null branches vanish. Specifying the action on the complement makes the recovery a total channel.

V33 / THE OPTIMAL SCALAR FOR TWO SPECTRAL POINTS

An approximate defect has a precise norm meaning

Traditional p. 58 / Definition II.8.6, Proposition II.8.7.

On a two-dimensional code, consider the overlap compression

$$A = PE_a^* E_b P = \mathrm{diag}(11/10, 9/10).$$

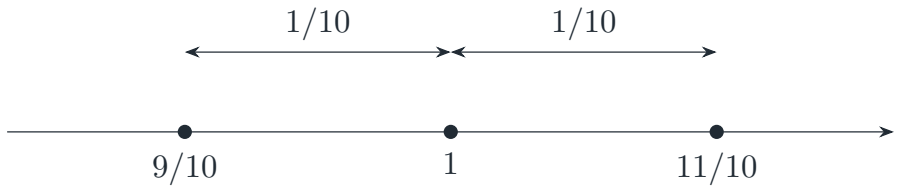
For instance, within the code take $E_a = I$ and $E_b = A$. This declares an error family, not by itself a normalized noise channel. The optimal scalar compression has

$$\inf_{c\in\mathbb{C}} \|A - cI\| = \frac{1}{10}, \qquad c = 1 \text{ attains it.}$$

Indeed, for every complex c, the triangle inequality gives

$$\frac{1}{5} = \left|\frac{11}{10} - \frac{9}{10}\right| \le \left|\frac{11}{10} - c\right| + \left|\frac{9}{10} - c\right|.$$

Thus the larger of the two distances is at least $1/10$, while both distances equal $1/10$ at $c = 1$.



one pair: $1/10$, full family $\{I, A\}$: $1/5$

What one pair contributes to the family defect

For unit code vectors ψ, ϕ, this pair therefore satisfies

$$|\langle E_a\psi, E_b\phi\rangle - \langle\psi, \phi\rangle| \le \frac{1}{10}.$$

The bound is attained on either coordinate vector. For the *whole* declared family $\{I, A\}$, the A^*A compression also enters the maximum: its diagonal entries are $121/100, 81/100$, giving pair defect $1/5$. Hence the full family value is $\varepsilon_{\mathrm{KL}} = 1/5$, not $1/10$.

This distinction prevents a tempting shortcut from one favorable overlap to an approximate correction claim. The quantity measures how close all overlap operators are to scalar action on the code. A recovery fidelity bound requires a declared normalized channel, a metric, and a separate continuity result.

What is checked exactly

For $\varepsilon \in \{0, 1/10, 1/4, 1\}$ the script checks $(A - I)^*(A - I) = \varepsilon^2 I$ for $A = \mathrm{diag}(1 + \varepsilon, 1 - \varepsilon)$ and several rational scalar controls. The triangle argument proves the lower bound for every complex scalar. Checking a finite list of candidates would not establish that conclusion. The family maximum above is also recorded separately.

> **Read this as:** An overlap norm has a useful operational interpretation. Evaluate every error pair, then keep that statement separate from an unproved recovery fidelity estimate.

V34 / SIGN, STABILITY, AND A CONVERGENT EXPANSION

Control the hidden spectral response

Traditional pp. 61, 65 / Theorem II.9.4, Proposition II.9.5, Theorem II.9.12.

Retain one coordinate in $H = \begin{pmatrix} 0 & 1 \\ 1 & 2 \end{pmatrix}$, so $A = 0$, $B = 1$, and $D = 2$. In its elimination domain, $\Sigma(z) = 1/(z-2)$. At $z = 3 + \mathrm{i}$,

$$\Sigma(3+\mathrm{i}) = \frac{1-\mathrm{i}}{2}, \qquad \Im\Sigma(z) = -(\Im z)\left|(z-2)^{-1}\right|^2 \le 0.$$

The sign in the upper half plane comes from self-adjoint hidden data. It is not an entrywise sign condition on an arbitrary effective matrix.

$$\boxed{\begin{array}{c} B = 1,\ D = 2 \\ \Sigma(3) = 1 \end{array}} \quad \longleftrightarrow \quad \boxed{\begin{array}{c} \widetilde{B} = 9/8,\ \widetilde{D} = 17/8 \\ \widetilde{\Sigma}(3) = 81/56 \end{array}}$$

$$25/56 \le 21/32$$

common hypotheses: $g = 9/8$, $\delta = 3/4$

A stability estimate with a common spectral gap

Compare $(B, D) = (1, 2)$ with $(\widetilde{B}, \widetilde{D}) = (9/8, 17/8)$ at $z = 3$. Both hidden spectral distances are at least $\delta = 3/4$, and both couplings are bounded by $g = 9/8$. Then

$$|\Sigma - \widetilde{\Sigma}| = \left|1 - \frac{81}{56}\right| = \frac{25}{56}, \qquad \frac{2g}{\delta}|B - \widetilde{B}| + \frac{g^2}{\delta^2}|D - \widetilde{D}| = \frac{21}{32}.$$

The theorem bounds the difference using a common spectral gap. Applying the bound uniformly to a refinement family requires uniform spectral separation and control of the couplings.

A series near zero energy and its exact remainder

At $z = 1/2$, $|z|\,|D^{-1}| = 1/4 < 1$, so

$$\Sigma(z) = -\sum_{n=0}^{\infty} \frac{z^n}{2^{n+1}}.$$

After the first four terms, the exact remainder has magnitude $1/384$. The geometric series controls the infinite tail. The retained check verifies that remainder, the complex sign identity, and the identities for the projected resolvent and bare truncation at four specified real spectral parameters.

At $z = 2$ the hidden inverse fails. At an eigenvalue of the full Hamiltonian, the retained Feshbach inverse fails. Neither point belongs to the resolvent identity's domain. Analytic continuation of a scalar expression does not erase its theorem hypotheses.

> **Read this as:** A uniform effective response requires a uniform gap and coupling bound. Exact small examples show how those hypotheses enter each estimate.

V35 / TWO HIDDEN FREQUENCIES AND A TEST OF LOCAL CLOSURE

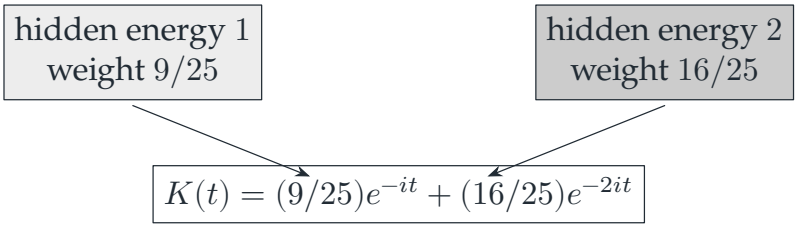
Memory positivity is a Gram identity

Traditional pp. 63, 64 / Theorem II.9.9, Theorem II.9.11.

Use retained space $\mathbb{C}$ and hidden space $\mathbb{C}^2$, with $A = 0$, $B = (3/5, 4/5)$, and $D = \operatorname{diag}(1, 2)$. The full Hamiltonian is $\begin{pmatrix} 0 & 3/5 & 4/5 \\ 3/5 & 1 & 0 \\ 4/5 & 0 & 2 \end{pmatrix}$. Its memory kernel is

$$K(t) = \frac{9}{25}e^{-\mathrm{i}t} + \frac{16}{25}e^{-2\mathrm{i}t}, \qquad K(0) = 1.$$

Each oscillatory coefficient is positive although $K(t)$ need not be real or pointwise nonnegative. At $t = \pi/2$, it equals $-16/25 - 9\mathrm{i}/25$.



Positive definite means a matrix test at arbitrary times

For retained scalars v_j and real times t_j, the structural identity is

$$\sum_{j,k} \overline{v}_j K(t_j - t_k) v_k = \left\| \sum_k e^{\mathrm{i}t_k D} B^* v_k \right\|^2 \geq 0.$$

The exact worked check specializes to $t = (0, \pi/2, \pi)$ and $v = (1, 2, -1)$. Its phases lie in $\mathbb{Q}(\mathrm{i})$, so both sides are computed without evaluating trigonometric functions. This Gram test illustrates the factorization. The written identity proves positivity for all choices of times and vectors.

Why this does not close to a bare local equation

With hidden initial state zero, the full system has $\ddot{x}(0) = -(A^2 + BB^*)x(0) = -x(0)$. The bare retained equation $\mathrm{i}\dot{x} = Ax$ would instead give zero acceleration. Therefore exact local closure for every retained initial state fails. More generally, equality of these accelerations forces $BB^* = 0$ and hence $B = 0$.

A nonzero initial hidden vector also supplies the forcing term $Be^{-\mathrm{i}tD}y(0)$. It is additional data, not part of the convolution kernel. The retained checks cover the displayed kernel values, exact Gram factorization, and acceleration defect. The integral equation follows from the written elimination argument.

> **Read this as:** Memory is positive definite through a Gram factorization, not through pointwise signs. Exact bare local closure requires the coupling to vanish.

V36 / STRICT POSITIVITY AND THE GROUND GAP

A positive transfer determines its Hamiltonian

Traditional pp. 66, 67 / Theorem II.10.2, Proposition II.10.5.

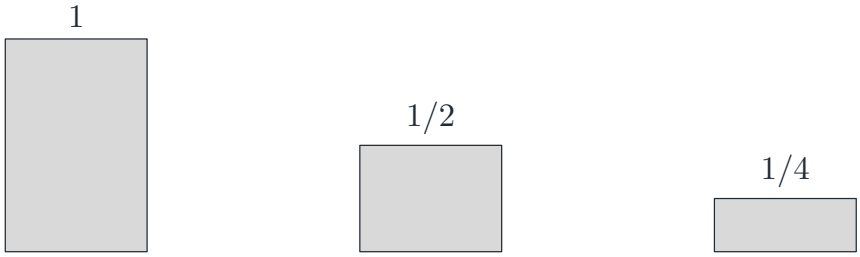
On $\mathcal{H} = \mathbb{C}^3$, take the strictly positive contraction

$$T = \operatorname{diag}(1, 1/2, 1/4), \qquad H = -\log T = \operatorname{diag}(0, \log 2, 2\log 2).$$

At unit Euclidean time, $T = e^{-H}$. The self-adjoint logarithm is unique because the logarithm acts on positive spectral values. At integer time $n \geq 0$,

$$T^n = \operatorname{diag}(1, 2^{-n}, 4^{-n}), \qquad P_0 = \operatorname{diag}(1, 0, 0), \qquad \|T^n - P_0\| = 2^{-n}.$$

The gap $\Delta = \log 2$ determines the rate $e^{-n\Delta}$ exactly in this example.



Strict positivity is an essential finite hypothesis

For $T' = \operatorname{diag}(1, 0)$, the operator is positive semidefinite, but there is no finite self-adjoint H' on all of $\mathbb{C}^2$ with $T' = e^{-H'}$: every finite eigenvalue of H' exponentiates to a strictly positive value. One may restrict to the positive support, but that changes the space on which the logarithm is defined.

For a family with nontrivial excited spectra, a uniform exponential rate needs a common positive lower bound on the gap. Ground multiplicity does not cause a problem: P_0 selects the entire eigenspace at the minimum energy. For a Hamiltonian whose minimum is $E_0 \neq 0$, the normalized transfer is $e^{-t(H-E_0 I)}$ before taking the limit.

Positivity is retained at several Euclidean times

For arbitrary vectors u_j and nonnegative integer times n_j, the reflected kernel obeys

$$\sum_{j,k} \langle u_j, T^{n_j+n_k} u_k \rangle = \left\| \sum_j T^{n_j} u_j \right\|^2 .$$

This is a finite Gram factorization. The retained run checks the integer semigroup and diagonal ground error for $n = 0, \ldots, 12$, and rejects a logarithm on the full space for the singular control. The written spectral argument justifies the logarithms and extends the functional calculus statement to all times.

> **Read this as:** A positive definite transfer can be logarithmically reconstructed. Ground convergence needs a declared normalization and gap, while continuum reconstruction still needs its own structure.

V37 / FINITE HEAT DATA AND THE QUANTIFIERS

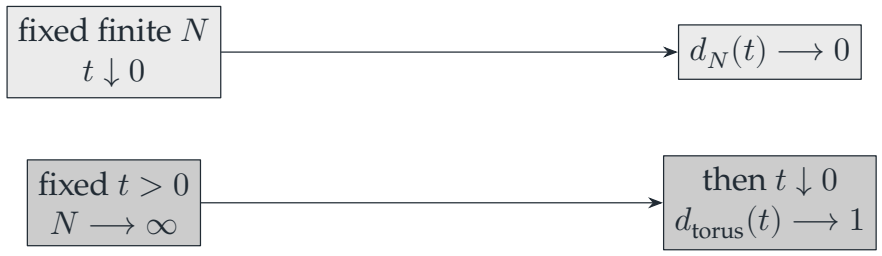
The dimension window has an order of limits

Traditional pp. 69, 70 / Theorem II.11.5, Corollary II.11.8.

For the unit circle grid with N sites, the scaled eigenvalues are $\lambda_N(k) = 4N^2 \sin^2(\pi k/N)$. Put $Z_N(t) = \sum_k e^{-t\lambda_N(k)}$ and $d_N(t) = 2t \sum_k \lambda_N(k) e^{-t\lambda_N(k)}/Z_N(t)$.
At the single time $t = \log 2/16$, two small grids admit exact rational heat weights:

N	spectrum	Z_N	$\sum \lambda e^{-t\lambda}$	$d_N/\log 2$
2	$(0, 16)$	$3/2$	8	$2/3$
4	$(0, 32, 32, 64)$	$25/16$	20	$8/5$

These are unnormalized traces. Normalizing by N changes Z_N but leaves the logarithmic derivative at that fixed grid unchanged.



The theorem uses two separate choices

For each $\varepsilon > 0$, first choose a fixed positive time t_ε so that the continuum torus dimension differs from one by less than $\varepsilon/2$. Then choose N_ε so that every $N \geq N_\varepsilon$ differs from that continuum value by less than $\varepsilon/2$ at the *same time*. This proves one controlled intermediate time for all sufficiently fine grids.

It does not assert a uniform interval width from that argument, a moving time t_N with no extra estimates, or a dimension plateau at every scale. At fixed finite N, $d_N(t) \to 0$ as $t \downarrow 0$ and as $t \to \infty$. By contrast, first taking $N \to \infty$ at positive t and then taking $t \downarrow 0$ yields the continuum dimension.

Where the infinite tail is controlled

At a fixed time, the proof bounds centered modes below by $16k^2$ and above by $4\pi^2 k^2$. The summable Gaussian dominators control both the heat trace and its first moment. A finite grid table supplies neither those tails nor the quantifiers. The retained check verifies the two displayed spectra, rational weights, traces, and dimension coefficients. It also distinguishes the unscaled cycle with four sites from the scaled unit circle grid.

> **Read this as:** The strengthened window result proves convergence after fixing a suitable time. The exact table is a worked calculation, not its proof.

V38 / THE IMAGE OF AN ISOMETRY IS NOT THE WHOLE LEVEL

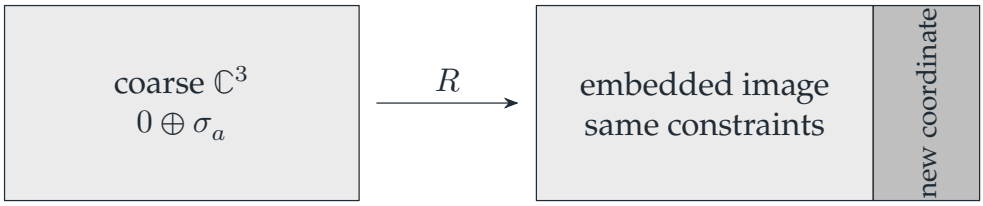
Transport constraints without hiding closure

Traditional pp. 71, 73 / Theorem II.12.2, Theorem II.12.5, Proposition II.12.6.

On $\mathbb{C}^3 = \mathbb{C}|0\rangle \oplus \mathbb{C}^2$, use $C_a = 0 \oplus \sigma_a$ for $a = x, y, z$. The common kernel is $\mathbb{C}|0\rangle$, and the full algebra closes:

$$[C_x, C_y] = 2\mathrm{i}C_z, \qquad [C_y, C_z] = 2\mathrm{i}C_x, \qquad [C_z, C_x] = 2\mathrm{i}C_y.$$

These are uncompressed identities. They supply an actual closure test in the quotient by the constraint span, unlike the automatic compressed zero on the physical kernel.



closure on im R transfers, and the new complement needs its own test

Exact transport holds on the coarse image

Embed by the coordinate isometry $R : \mathbb{C}^3 \to \mathbb{C}^4$ and set $\widetilde{C}_a = C_a \oplus 1$. Then $\widetilde{C}_a R = RC_a$, so

$$[\widetilde{C}_a, \widetilde{C}_b]R = R[C_a, C_b].$$

The coarse physical vector maps into the fine common kernel. However, the same prescribed Pauli structure does *not* close on the whole fine level: on the added coordinate the commutator is zero, whereas $2\mathrm{i}\widetilde{C}_z$ is $2\mathrm{i}$. Exact transport constrains the image of R and leaves its orthogonal complement as separate data.

An approximate residual is also explicit

Perturb only $\widetilde{C}_x$ by $(1/10)|0\rangle\langle 0|$. For the unit coarse physical vector, the fine constraint residual is exactly $1/10$. The intertwining defect has the same norm. The general result for approximate transport controls these residuals and commutator errors using the defect sizes and a common bound on the constraint norms. A nonzero anomaly remains an error that must be controlled.

The retained checks verify all three coarse commutators, the isometry, each constraint intertwining, all nine commutator transports, and the residual. The added coordinate provides a counterexample to extending the identity on the image to the whole space. Unbounded constraints would additionally require a common invariant domain.

> **Read this as:** Closure is a statement about the operator algebra. Refinement intertwining transports it to the embedded image. The new degrees of freedom require their own control.

V39 / EXACT EMBEDDINGS AND A SUMMABLE TAIL

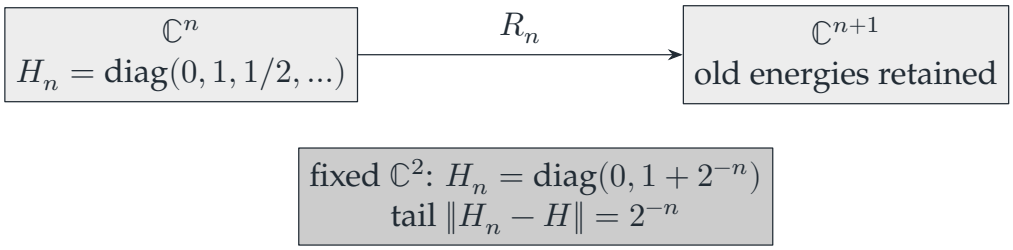
Two routes to a bounded Hamiltonian limit

Traditional pp. 75, 76 / Theorem II.13.2, Theorem II.13.4, Corollary II.13.5.

For the exact route, let $\mathcal{H}_n = \mathbb{C}^n$ with coordinate inclusions and

$$H_n = \operatorname{diag}(0, 1, 1/2, \dots, 1/(n-1)), \qquad H_1 = (0).$$

The old energies are retained at every level, $H_{n+1}R_n = R_nH_n$, and $\|H_n\| \le 1$. On the Hilbert space of the direct limit $\ell^2(\mathbb{N}_0)$, the diagonal sequence defines a bounded self-adjoint H_∞. Projectors onto even addresses also intertwine and give a fixed complete system of two packets in the limit.



Compatibility and boundedness are different assumptions

The equally compatible tower $\operatorname{diag}(0, 1, 2, \dots, n-1)$ has growing norms. It does not satisfy the bounded direct limit theorem. Its natural diagonal operator needs a separately specified domain. Dropping the uniform norm hypothesis does not supply that domain argument.

For the norm route, work instead on the *single fixed space* $\mathbb{C}^2$ and set

$$H_n = \operatorname{diag}(0, 1 + 2^{-n}), \qquad H = \operatorname{diag}(0, 1).$$

Here $\|H_{n+1} - H_n\| = 2^{-(n+1)}$ and $\|H_n - H\| = 2^{-n}$. The summable tail supplies an error bound for every n. For $|t| \le T$, the paper's Duhamel estimate gives

$$\left\|e^{-\mathrm{i}tH_n} - e^{-\mathrm{i}tH}\right\| \le T2^{-n}.$$

The Euclidean counterpart holds on $0 \le t \le T$ because both Hamiltonians are nonnegative. If packet projectors also converge in norm, leakage operators converge uniformly on these time intervals.

Execution scope

Exact inclusions and projector compatibility are checked through level eight. The two-dimensional tail identities are checked for $n = 0, \dots, 12$. Their infinite conclusion uses the displayed geometric series and the theorem's analytic estimate. A finite prefix cannot certify an unspecified continuation of a tower.

> **Read this as:** Exact embedded compatibility uses a uniform norm bound. Approximate convergence uses a common space and summable defects. Keep the hypotheses of these two routes explicit.

V40 / REFLECTION GRAMS, TRACES, AND FINAL SCOPE

Choose the topology that preserves the quantity

Traditional pp. 77, 78 / Theorem II.13.6, Theorem II.13.8, Section II.14.

Let $q_n = 1/2+2^{-(n+2)}$ and define the scalar reflected kernel $C_n(j,k) = 1+q_n^{j+k}$ on nonnegative integers. Each finite Gram matrix is a sum of two positive rank-one matrices, and pointwise convergence gives $C(j,k) = 1 + (1/2)^{j+k}$. For times $(0,1,2)$ and coefficients $(1,-2,1)$,

$$\sum_{j,k} v_j C_n(j,k) v_k = (1-q_n)^4 \geq 0.$$

This exact check illustrates how finite quadratic forms pass positivity to the limit.



positive trace-class control: norm convergence alone does not preserve a trace

Operator norm does not preserve trace in growing rank

On ℓ^2, let P_n select the first n coordinates and set $A_n = P_n/n$. Then $\|A_n\| = 1/n \to 0$ while $\operatorname{Tr} A_n = 1$ for every n. These positive trace-class operators show why the choice of topology matters. Their zero limit is not the heat operator of a finite Hamiltonian.

For transfers on two states $T_n = \operatorname{diag}(1, q_n) = e^{-H_n}$, with $H_n = \operatorname{diag}(0, -\log q_n)$ at unit time, the error in trace norm is $2^{-(n+2)}$ and the heat traces converge to $3/2$. The criterion for convergence of spectral dimension additionally assumes convergence of the first heat moments in trace norm and a nonzero limiting heat trace. Convergence of the heat trace alone does not determine that quotient.

The retained evidence and the remaining open targets

The extension includes retained exact checks over specified finite ranges in $\mathbb{Q}(\mathrm{i})$ using `Fraction` from Python's standard library. The original appendix's record of 180 checks, including symbolic derivatives, is also retained. Both records come from earlier executions. This prose revision adds no symbolic or Lean kernel run. All model and vector sources remain supplied.

The saved v0.6.0 ledger lists 19 finite items with their recorded hypotheses. Its five original targets for continuum and physical reconstruction remain open. The strengthened edition supplies analytic proofs and criteria for bounded limits. These results and examples do not establish the unresolved physical existence claims.

> **Read this as:** Use pointwise convergence for finite positivity tests, operator norm for bounded dynamics and constraints, and trace norm for heat traces. Every conclusion keeps its own hypotheses and evidence scope.